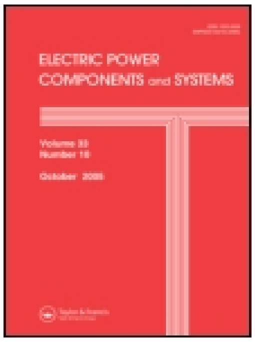

Electric Power Components and Systems

ISSN: 1532-5008 (Print) 1532-5016 (Online) Journal homepage: www.tandfonline.com/journals/uemp20

Wavelet ANN Based Stator Ground Fault Protection Scheme for Turbo Generators

Shaik Abdul Gafoor & P. V. Ramana Rao

To cite this article: Shaik Abdul Gafoor & P. V. Ramana Rao (2007) Wavelet ANN Based Stator Ground Fault Protection Scheme for Turbo Generators, Electric Power Components and Systems, 35:5, 575-590, DOI: 10.1080/15325000601078195

To link to this article: https://doi.org/10.1080/15325000601078195

Published online: 24 Feb 2007.

Electric Power Components and Systems, 35:575–590, 2007

ISSN: 1532-5008 print/1532-5016 online
DOI: 10.1080/15325000601078195

Wavelet ANN Based Stator Ground Fault Protection Scheme for Turbo Generators

SHAIK ABDUL GAFOOR

Electrical Engineering Department
National Institute of Technology
Warangal, India

P. V. RAMANA RAO

Electrical Engineering Department
National Institute of Technology
Warangal, India

Abstract *This article proposes a protection scheme for turbo generators to detect stator ground faults in particular closer to neutral. The scheme considers total generated voltage of the machine and makes use of wavelet multi-resolution analysis. A fault index is defined in terms of peak and valley values of the highest-level wavelet decomposition, which is compared with a threshold value to discriminate from other transients, like sudden unbalance, in load. To identify the faulty coil, an ANN employing back propagation algorithm is used with the lowest level wavelet coefficients as inputs. The results of digital simulation are presented for different fault impedances and fault locations.*

Keywords ground fault protection, multi-resolution analysis, fault index, threshold

1. Introduction

The normal operation of a generator, which is a vital component of a power system, is essential for ensuring reliability and quality of power supply. Turbo generators are subjected to mechanical stresses and electromagnetic impacts continuously and hence are likely to develop stator-winding faults. Among the generator faults, stator ground fault is the most common. Faults closer to neutral are critical in view of occurrence of a subsequent fault, which leads to inter-turn faults. Several schemes for detection of such faults are proposed using third harmonic voltages and sub-harmonic voltage injection [1–3]. Methods comparing magnitude and phase angle of neutral and terminal third harmonic voltages suffer from low sensitivity as they are dependent on the operating condition of the generator. Subharmonic injection method is expensive and fails in case of open circuit in neutral grounding. An adaptive method is proposed to overcome the problem of low sensitivity [4]. Wavelet based multi-resolution analysis (MRA) is an

Manuscript received 21 March 2006; accepted 4 October 2006.
Address correspondence to Mr. Shaik Gafoor, Electrical Engineering Dept., Warangal 506004, India. Email: saadgafoor@yahoo.com

ideal technique for analyzing the power system transients in general [5, 8] and generator protection in particular [7, 10]. Third harmonic neutral and terminal voltage signals are analyzed with the help of wavelet MRA to detect ground faults. Polarities of maximum modulii are compared to distinguish ground faults from other transients [10]. A third harmonic filter is required to feed the WT based protection scheme. The scheme is affected by the performance of third harmonic filters.

In the proposed work, the total generated neutral and terminal voltages of the machine (containing fundamental component and 3rd harmonics) are analyzed with the help of MRA both in frequency and time domains thereby eliminating the need of extracting third harmonic contents. A fault index computed from the finer level decomposition is used to detect the transients, and is compared with a threshold value. This also discriminates from other transients like sudden unbalance in load. The proposed method is found to be effective in detecting faults closer to neutral as well as high impedance faults. The advantage of the proposed scheme is better sensitivity for high impedance fault compared to solid faults. The approximate coefficients of neutral voltage MRA are then used as inputs to an ANN for identifying the faulty coil. Back propagation algorithm is used for this purpose. The article is organized as follows. Section 2 presents general introduction of wavelet transforms. Section 3 deals with the detection of fault based on wavelet MRA. Section 4 illustrates the faulty coil detection using ANN, and conclusions are presented in Section 5.

2. Wavelet Analysis

Wavelet transform (WT) is an efficient means of analyzing transient currents and voltages. Unlike DFT, WT not only analyzes the signal in frequency bands but also provides non-uniform division of frequency domain, *i.e.*, WT uses short window at high frequencies and long window at low frequencies. This helps to analyze the signal in both frequency and time domains effectively. A set of basis functions called wavelets are used to decompose the signal in various frequency bands, which are obtained from a mother wavelet by dilation and translation. Hence, the amplitude and incidence of each frequency can be found precisely.

Wavelet transform is defined as a sequence of a function $\{h(n)\}$(low pass filter) and $\{g(n)\}$(high pass filter). The scaling function $\varphi(t)$ and wavelet $\psi(t)$ are defined by the following equations.

$$\varphi(t) = \sqrt{2}\sum h(n)\varphi(2t - n)$$

$$\psi(t) = \sqrt{2}\sum g(n)\varphi(2t - n)$$

where $g(n) = (-1)^n h(1 - n)$.

A sequence of $\{h(n)\}$ defines a wavelet transform. There are many types of wavelets such as Haar, Daubachies, and Symlet, etc. The selection of mother wavelet is based on the type of application [5].

3. Ground Fault Detection

The ground fault protection scheme of the generator depends on its terminal connections and how its neutral is grounded. In this article, a turbo generator connected to a step up transformer, unit auxiliary transformer, and a voltage transformer is considered, as shown in Figure 1. The neutral of the generator is grounded through a distribution transformer with resistance-loaded secondary. The generator has two poles and 36 slots and 6 coils per phase with 8 turns per coil [2]. Thus, each turn covers 2.08% of total winding. The generator winding is modeled as 48 pi-sections connected in cascade using MATLAB. Each pi-section represents a turn. The pi-section is connected in series with a voltage source containing fundamental and harmonics, as shown in Figure 2. The proposed scheme makes use of the total generated voltage in the machine instead of only the generated third harmonics [10], thus avoiding the need of extracting third harmonic content from the generated voltage. Several wavelets have been tried for the analysis in the laboratory and bi-orthogonal 6.8 is found to be the most suitable mother wavelet for the proposed scheme. Neutral and terminal voltages are sampled, at 7.2 kHz and any changes in the smoothness of the signals are analyzed at finer level to detect the ground fault.

The neutral voltage under normal operation is due to charging current caused by generated third harmonic voltages only, as the charging currents due to balanced fundamental component of generated voltages sum up to zero. This is shown in Figure 3. When a ground fault occurs, fundamental component of the terminal voltage (with very

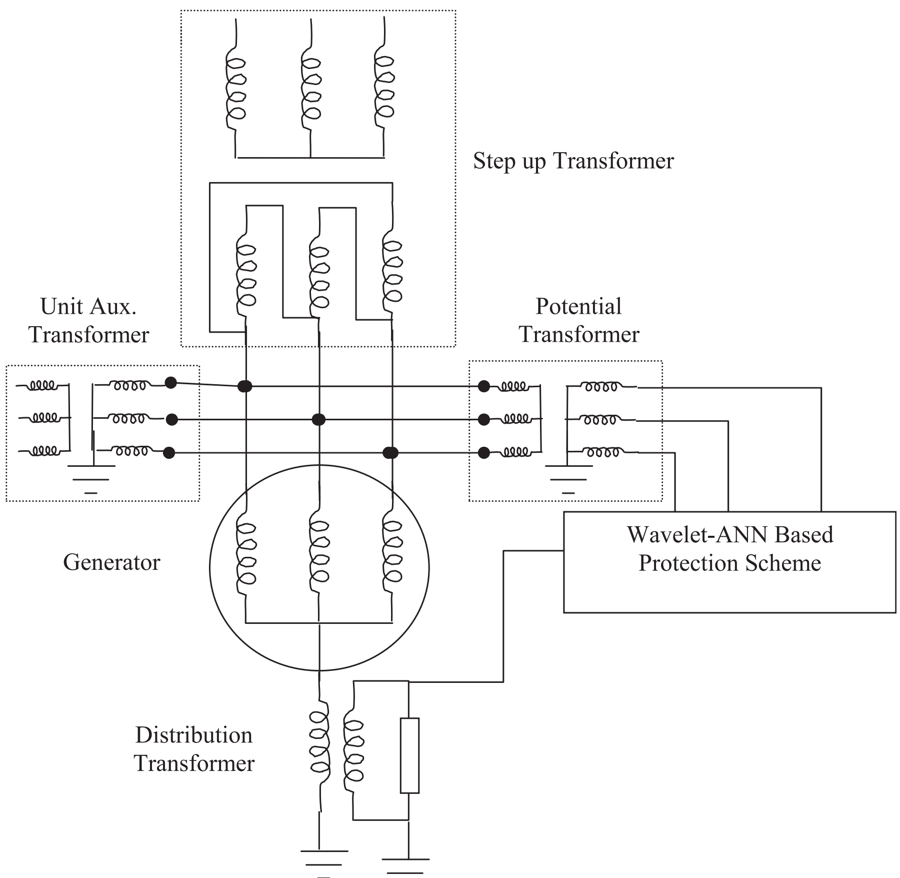

Figure 1. Conventional unit type connection.

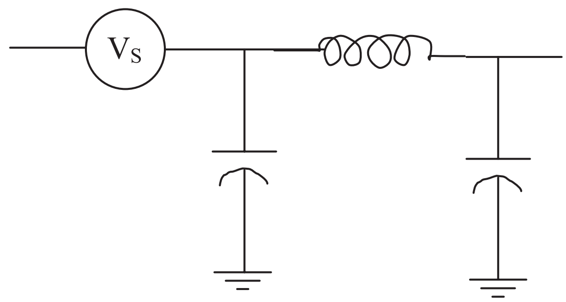

V_S: Voltage source containing fundamental and third harmonics.

Figure 2. Pi-model of each turn.

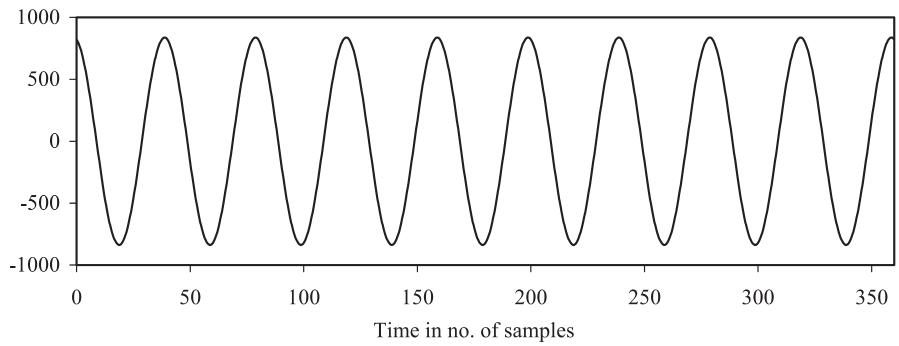

Figure 3. Neutral voltage under normal operation.

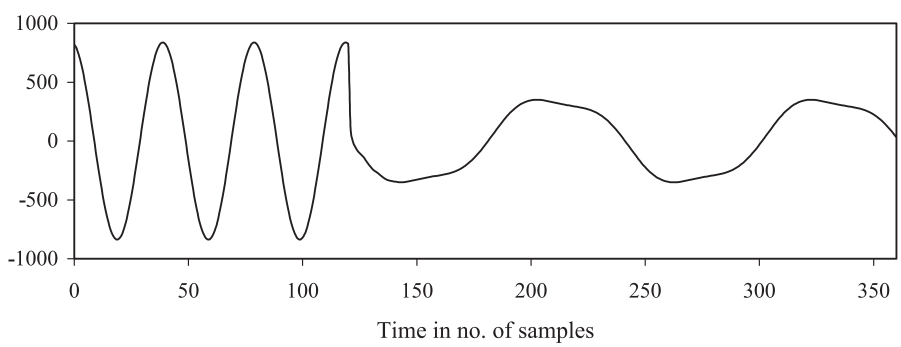

Figure 4. Neutral voltage under ground fault at $\alpha = 2.08$.

low content of third harmonic) is superimposed on the existing third harmonic neutral voltage, due to fault current flowing in the neutral. The resulting waveform is illustrated in Figure 4. Fault location α is defined as the percentage of number of turns between the neutral and the fault location to the total turns of the winding. As the fault location moves towards the terminal, the fundamental component of the neutral increases due to increase in fault current. This is illustrated in Figures 5–7.

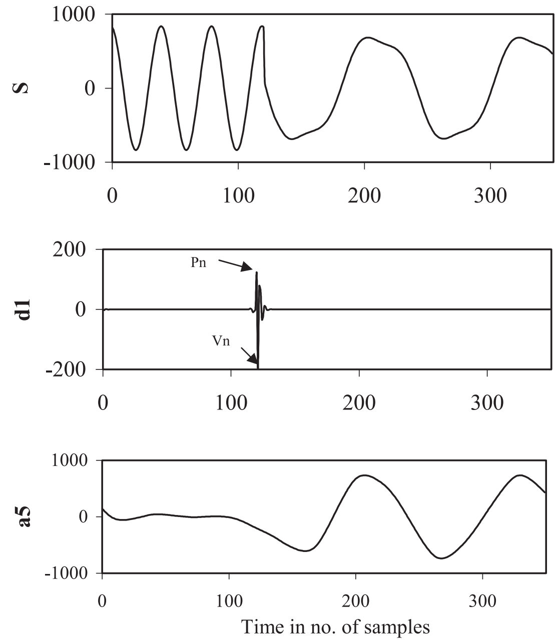

(a)

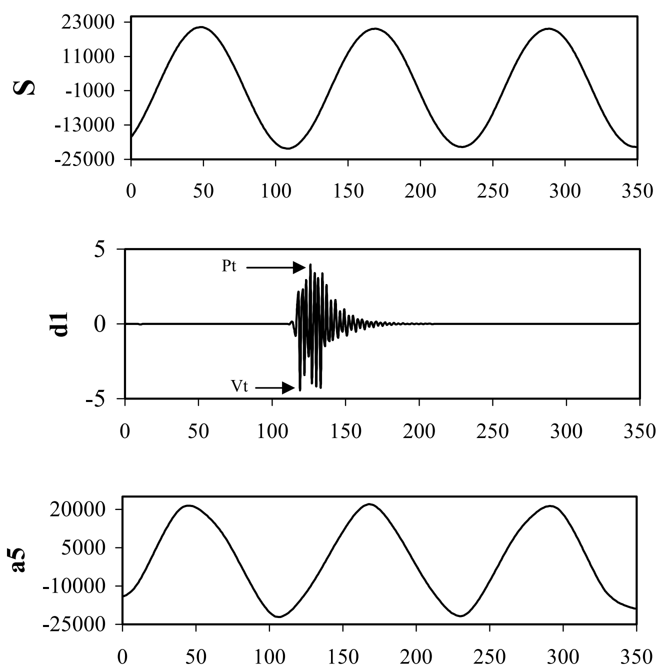

(b)

Figure 5. (a) Decomposition of neutral voltage for $\alpha = 4.17\%$; and (b) decomposition of terminal voltage for $\alpha = 4.17\%$.

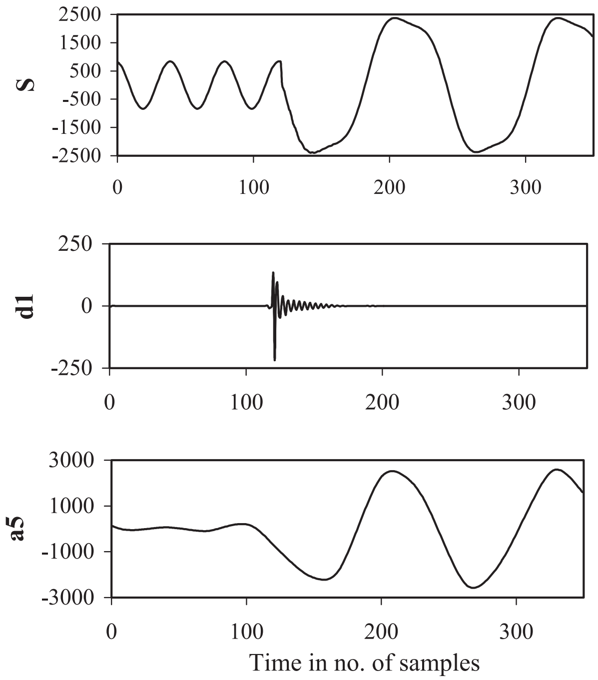

(a)

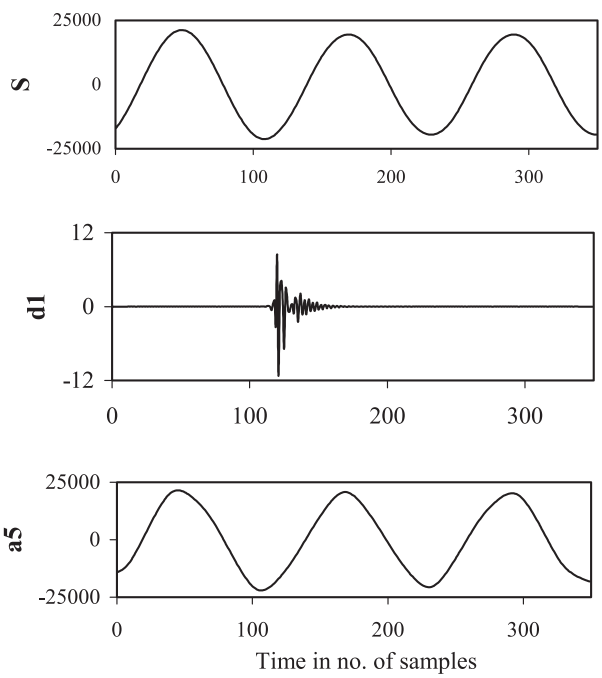

(b)

Figure 6. (a) Decomposition of neutral voltage for $\alpha = 16.7\%$; and (b) decomposition of terminal voltage for $\alpha = 16.7\%$.

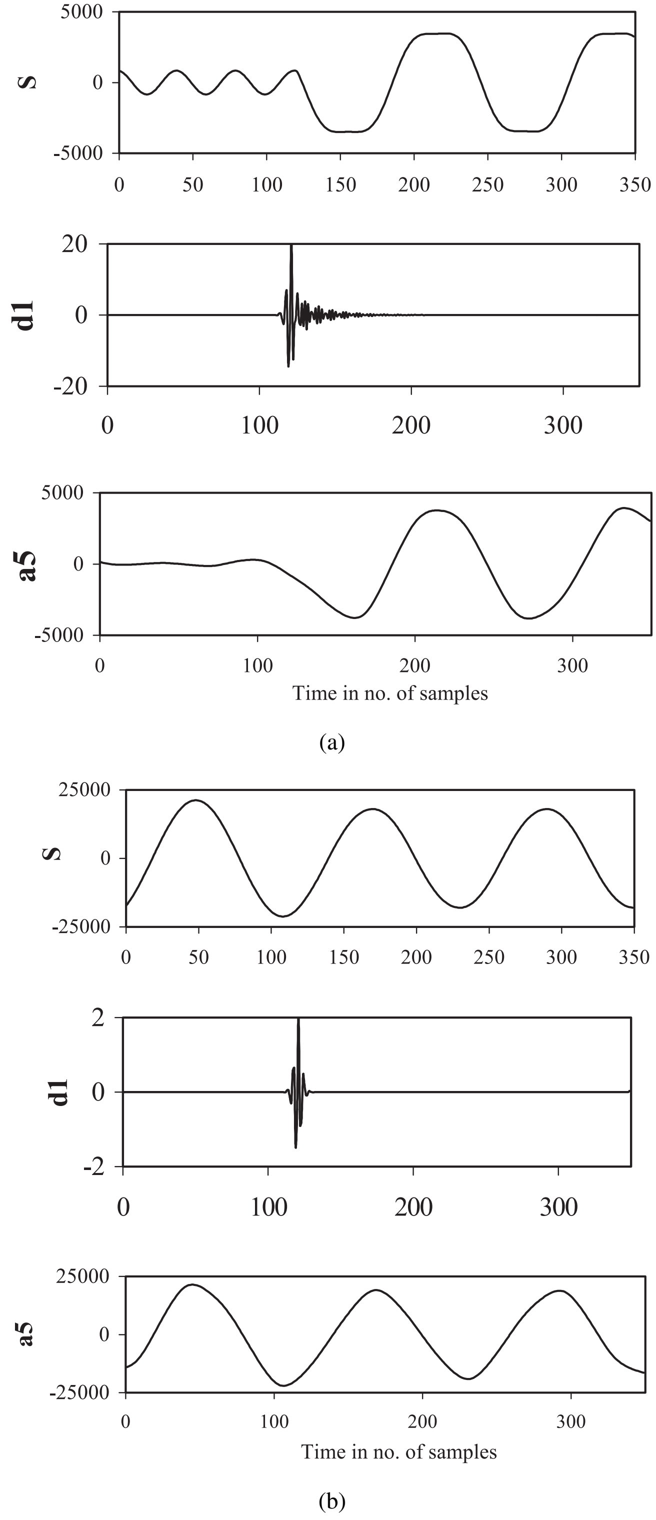

Figure 7. (a) Decomposition of neutral voltage for $\alpha = 29.2\%$; and (b) decomposition of terminal voltage for $\alpha = 29.2\%$.

The transients associated with the fault are characterized by the frequency contents. The terminal voltage has predominant fundamental component, whereas the fundamental component of the neutral voltage increases with fault the location α. The transients of neutral and terminal voltages are analyzed using wavelet based MRA, as plotted in Figures 5–7, for various values of α. **S** indicates the sampled signal (neutral/terminal voltage), $\mathbf{d_1}$, the finer level decomposition (3.6 kHz–1.8 kHz) and $\mathbf{a_5}$, the coarser level decomposition (225 Hz–0 Hz). From Figures 5(a) and 5(b) ($\alpha = 4.17\%$), it can be observed that $\mathbf{d_1}$ level decompositions of neutral and terminal voltages are different. This is due to large difference in percentage third harmonic content in these two voltages. The per unit peak values and valley values differ much. However, for higher values of α (16.7% and 29.2%) $\mathbf{d_1}$ level decomposition of these two voltages tend to resemble each other, as evident from the Figures 6(a), 6(b), and 7(a), 7(b). From these figures, it is observed that the per unit peak values and valley values of neutral and terminal voltages are approximately the same. This is so since the percentages of third harmonic content of both neutral and terminal voltages are approximately equal. It is thus evident from Figures 5–7 that the variations in per unit peak and valley values of d1-level decompositions are dependent on percentage third harmonic content of neutral and terminal voltages. These peak and valley values of $\mathbf{d_1}$-level decompositions are used to define a fault index ($\in$) which is further utilized to detect ground fault. The fault index $\in$ is defined as

$$\in = \sqrt{(p_t - p_n)^2 + (v_t - v_n)^2}$$

where

$$p_n = Pn/(Pn - Vn)$$

$$v_n = Vn/(Pn - Vn)$$

$$p_t = P_t/(Pt - Vt)$$

$$v_t = V_t/(Pt - Vt)$$

(Pn, Vn) and (Pt, Vt) are peak and valley values of $\mathbf{d_1}$ decomposition of neutral and terminal voltages respectively. The fault index $\in$ decreases with increase in α, as shown in Figure 8, due to similarities in the $\mathbf{d_1}$-decopositions of neutral and terminal voltages. This leads to a minimum value of fault index called threshold (**Th**) corresponding to $\alpha = 100\%$. Thus, for stator ground faults at any location α, the fault index $\in$ is greater than or equal to threshold **Th**. Hence, faults closer to neutral can be easily detected. Ground faults with considerable fault impedance limit the neutral current. Hence, the fundamental component of neutral voltage decreases with increase in fault impedance. This leads to a considerable difference in third harmonic contents of neutral and terminal voltages. Consequently, the fault index will have higher values compared to solid ground faults, as shown in Figure 9. Thus, the above scheme also provides effective protection against high impedance faults.

A sudden unbalance in load may lead to similar transients in neutral and terminal voltages and should be discriminated from ground faults. The former can be reviewed as an external fault with finite impedance, and is discriminated with the help of fault index. The fault index of these transients varies, as shown in Figure 10, for

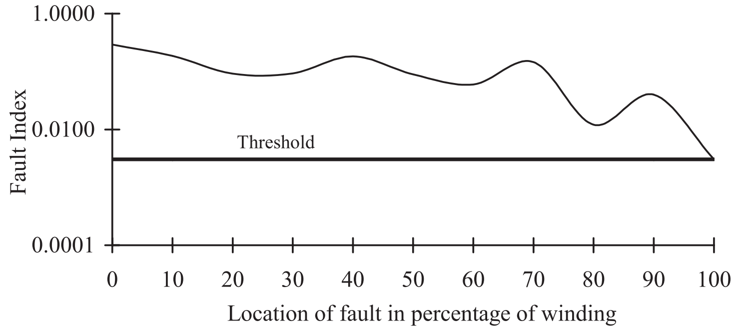

Figure 8. Variation of fault index with fault location (Zf = 0 Ω).

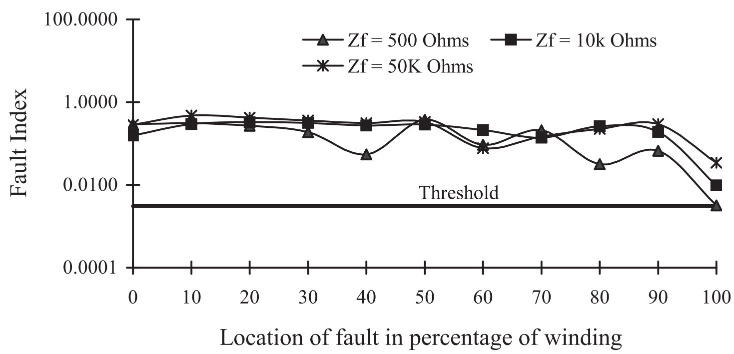

Figure 9. Variation of fault index with fault location for various Zfs.

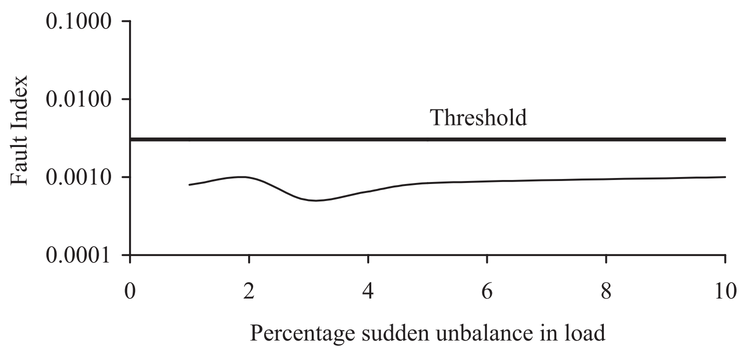

Figure 10. Variation of fault index with percentage sudden unbalance in load.

different percentages of unbalance. The fault index for sudden unbalance in load is always less than the threshold value set for ground fault, and thus it can be distinguished easily.

4. ANN Based Faulty Coil Identification

Artificial neural networks, which are efficient tools for pattern recognition and classification, can also be used effectively in power system protection [6, 9]. In this work, a feed

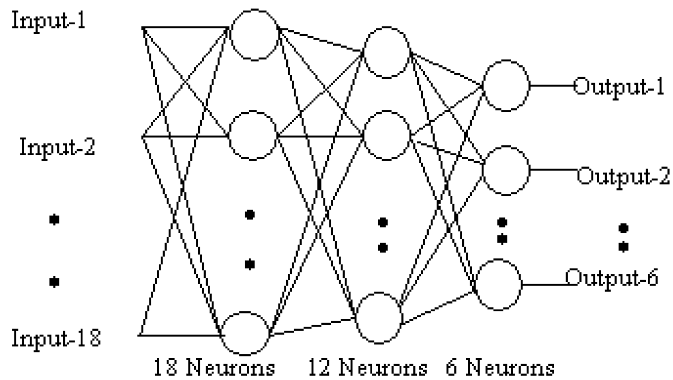

Figure 11. Architecture of the ANN considered.

forward neural network (FNN) is used to identify the faulty coil in the stator winding. This FNN is fed with approximate coefficients of 5th level decomposition of neutral voltage as inputs. It can observed from Figures 5(a), 6(a) and 7(a) that amplitude of 5th level approximate decomposition of neutral voltage signal ($\mathbf{a_5}$) (after the incidence of fault) increases with the fault location. Hence, the $\mathbf{a_5}$ coefficients of the neutral voltage are obtained for two cycles after the incidence of fault are used as inputs to the feed forward neural network (FNN) to detect the faulty coil. The eighteen $\mathbf{a_5}$ coefficients obtained from the 5th level approximate decomposition of neutral voltage forms the input vector to FNN.

FNN consist of 18 neurons in the input layer, 12 neurons in the hidden layer and 6 neurons in the output layer, as shown in Figure 11. The output O_i goes high ($O_i = 1.0$) for a fault in the ith coil. Each coil covers 16.67% of total winding. The proposed FNN is simulated using MATLAB software. Table 1 shows the training input data obtained by simulating faults at various locations of generator winding. Table 2 shows corresponding target data for the neural network. The trained FNN is tested, by simulating faults at new locations, and the test input data is shown in Table 3. The corresponding output of FNN is presented in Table 4. From Table 4, it can be seen that the outputs differ from their targets for faults only at the boundaries of two adjacent coils. Since outputs are very close to their target values, identification of faulty coil is fairly accurate. Table 5 shows errors in the identification of faulty coil.

5. Conclusions

This article introduces wavelet decomposition method for analyzing the transients of the total generated neutral and terminal voltages in the event of a stator ground fault, thereby eliminating need of third harmonic filters. A fault index based on finer level decomposition of these two voltages is used to detect ground faults closer to neutral and high impedance faults. The scheme provides inherent discrimination from sudden unbalance in loads. The approximate coefficients of fifth level decomposition of the neutral voltage alone are used to identify the faulty coil with the help of an artificial neural network.

Table 1
Training input data

	Location of fault											
	Coil-1		Coil-2		Coil-3		Coil-4		Coil-5		Coil-6	
Inputs	4.2%	12.5%	20.8%	29.2%	37.5%	45.8%	54.2%	62.5%	70.8%	79.2%	87.5%	91.7%
1	0.008	0.008	0.007	0.007	0.007	0.007	0.008	0.008	0.009	0.009	0.010	0.010
2	0.014	0.021	0.025	0.027	0.027	0.026	0.023	0.020	0.016	0.013	0.005	0.001
3	−0.006	−0.015	−0.025	−0.031	−0.033	−0.031	−0.026	−0.020	−0.010	−0.004	0.015	0.023
4	−0.001	0.016	0.051	0.083	0.110	0.132	0.147	0.166	0.172	0.173	0.169	0.164
5	−0.007	−0.713	−1.020	−1.179	−1.210	−1.140	−0.981	−0.735	−0.433	−0.251	0.330	0.558
6	0.019	−0.752	−1.286	−1.849	−2.408	−2.955	−3.467	−3.951	−4.384	−4.586	−5.113	−5.262
7	0.279	0.968	1.362	1.585	1.654	1.597	1.428	1.168	0.825	0.616	−0.054	−0.318
8	0.194	0.513	0.953	1.459	1.992	2.539	3.075	3.598	4.090	4.329	4.976	5.174
9	−0.396	−1.064	−1.547	−1.871	−2.048	−2.104	−2.045	−1.893	−1.653	−1.494	−0.962	−0.740
10	−0.091	−0.289	−0.630	−1.071	−1.571	−2.112	−2.666	−3.227	−3.776	−4.052	−4.820	−5.068
11	0.394	1.079	1.612	2.015	2.288	2.452	2.511	2.481	2.364	2.268	1.915	1.753
12	0.146	0.437	0.851	1.350	1.891	2.460	3.029	3.594	4.136	4.404	5.143	5.377
13	0.135	0.404	0.803	1.290	1.823	2.386	2.952	3.516	4.059	4.328	5.069	5.305
14	0.122	0.372	0.758	1.240	1.774	2.342	2.918	3.494	4.053	4.331	5.103	5.350
15	0.129	0.390	0.782	1.266	1.799	2.363	2.933	3.501	4.050	4.323	5.077	5.317
16	0.122	0.369	0.754	1.233	1.764	2.329	2.901	3.474	4.029	4.305	5.071	5.315
17	0.128	0.386	0.777	1.260	1.793	2.359	2.929	3.500	4.051	4.325	5.084	5.326
18	0.131	0.396	0.793	1.280	1.816	2.384	2.956	3.527	4.077	4.351	5.106	5.346

Table 2
Target data

	Location of fault											
	Coil-1		Coil-2		Coil-3		Coil-4		Coil-5		Coil-6	
Outputs	4.2%	12.5%	20.8%	29.2%	37.5%	45.8%	54.2%	62.5%	70.8%	79.2%	87.5%	91.7%
1	1	1	0	0	0	0	0	0	0	0	0	0
2	0	0	1	1	0	0	0	0	0	0	0	0
3	0	0	0	0	1	1	0	0	0	0	0	0
4	0	0	0	0	0	0	1	1	0	0	0	0
5	0	0	0	0	0	0	0	0	1	1	0	0
6	0	0	0	0	0	0	0	0	0	0	1	1

Table 3
Test input data

	Location of fault											
	Coil-1		Coil-2		Coil-3		Coil-4		Coil-5		Coil-6	
Inputs	2.1%	10.4%	18.7%	27.1%	35.4%	43.7%	52.1%	60.4%	68.7%	77.1%	81.2%	89.6%
1	0.009	0.008	0.007	0.007	0.007	0.007	0.007	0.008	0.008	0.009	0.010	0.010
2	0.012	0.019	0.024	0.026	0.027	0.026	0.024	0.021	0.017	0.012	0.006	0.003
3	0.005	−0.011	−0.024	−0.030	−0.033	−0.031	−0.028	−0.022	−0.013	−0.001	0.011	0.019
4	−0.032	0.007	0.042	0.076	0.104	0.128	0.146	0.164	0.170	0.173	0.169	0.166
5	−0.076	−0.599	−0.974	−1.142	−1.229	−1.156	−1.043	−0.791	−0.529	−0.157	0.208	0.445
6	−0.149	−0.637	−1.133	−1.716	−2.259	−2.825	−3.338	−3.837	−4.278	−4.683	−5.034	−5.189
7	0.188	0.828	1.296	1.535	1.665	1.613	1.496	1.231	0.933	0.514	0.082	−0.187
8	0.087	0.429	0.817	1.339	1.844	2.409	2.933	3.473	3.965	4.443	4.872	5.077
9	−0.201	−0.909	−1.453	−1.797	−2.030	−2.092	−2.084	−1.931	−1.735	−1.417	−1.076	−0.850
10	−0.044	−0.238	−0.512	−0.965	−1.425	−1.983	−2.515	−3.093	−3.632	−4.184	−4.691	−4.946
11	0.201	0.919	1.498	1.921	2.240	2.415	2.517	2.489	2.413	2.221	1.998	1.833
12	0.073	0.365	0.717	1.231	1.737	2.325	2.876	3.459	3.996	4.533	5.021	5.262
13	0.067	0.337	0.671	1.173	1.670	2.252	2.800	3.381	3.918	4.456	4.947	5.189
14	0.061	0.309	0.629	1.125	1.620	2.207	2.762	3.357	3.908	4.465	4.974	5.228
15	0.064	0.325	0.652	1.150	1.646	2.229	2.779	3.366	3.908	4.454	4.952	5.199
16	0.060	0.307	0.625	1.118	1.610	2.194	2.746	3.337	3.884	4.437	4.943	5.194
17	0.064	0.321	0.647	1.145	1.640	2.224	2.775	3.364	3.908	4.456	4.958	5.206
18	0.065	0.330	0.661	1.164	1.663	2.249	2.801	3.390	3.934	4.481	4.981	5.228

Table 4
Output of FNN

	Location of fault											
	Coil-1		Coil-2		Coil-3		Coil-4		Coil-5		Coil-6	
Outputs	2.1%	10.4%	18.7%	27.1%	35.4%	43.7%	52.1%	60.4%	68.7%	77.1%	81.2%	89.6%
1	**1**	**1**	0.11	0	0	0	0	0	0	0	0	0
2	0	0	**0.98**	**1**	0	0	0	0	0	0	0	0
3	0	0	0	0	**1**	**1**	0	0	0	0	0	0
4	0	0	0	0	0	0	**0.98**	**1**	0	0	0	0
5	0	0	0	0	0	0	0	0	**1**	**1**	0.04	0
6	0	0	0	0	0	0	0	0	0	0	**0.92**	**1**

Table 5
Errors in fault identification

	Location of fault											
	Coil-1		Coil-2		Coil-3		Coil-4		Coil-5		Coil-6	
Outputs	2.1%	10.4%	18.7%	27.1%	35.4%	43.7%	52.1%	60.4%	68.7%	77.1%	81.2%	89.6%
1	0	0	**−0.11**	0	0	0	0	0	0	0	0	0
2	0	0	**0.02**	0	0	0	0	0	0	0	0	0
3	0	0	0	0	0	0	**−0.01**	0	0	0	0	0
4	0	0	0	0	0	0	**0.02**	0	0	0	0	0
5	0	0	0	0	0	0	0	0	0	0	**−0.04**	0
6	0	0	0	0	0	0	0	0	0	0	**0.08**	0

References

1. Schlake, R. L., Buckley, G. W., and McPherson, G., "Performance of third harmonic ground fault protection scheme for generator stator winding," *IEEE Trans. on Power Apparatus and Systems*, PAS-100, No. 7, pp. 3195–3202, July 1981.
2. Pope, J. W., "A comparison of 100% stator ground fault protection scheme for generator stator windings," *IEEE Trans. on Power Apparatus and Systems*, Vol. PAS-103, No. 4, pp. 832–840, April 1984.
3. Mattila, R. J., "Design principles of a new generator stator ground relay for 100% coverage of stator winding," *IEEE Trans. on Power Delivery*, Vol. PWRD-1 No. 4, pp. 41–51, October 1986.
4. Yin, X. G., Malik, O. P., Hope, G. S., and Chen, D. S., "Adaptive ground fault protection schemes for turbo generators based on third harmonic voltages," *IEEE Trans. on Power Delivery*, Vol. 5, No. 2, pp. 595–603, April 1990.
5. Galli, A. W., Heydt, G. T., and Ribeiro, P. F., "Exploring the power of wavelet analysis," *IEEE Computer Applications in Power*, pp. 37–41, October 1996.
6. Megahid, A. I., and Malik, O. P., "An artificial neural network based digital differential protection scheme for synchronous generator stator winding protection," *IEEE Trans. on Power Delivery*, Vol. 14, No. 1, pp. 86–93, January 1999.
7. Goupci, W., Laguna, Zhen, R., and Qungu, H., "A novel method for large turbine generator protection based on wavelet transformation," *Proceedings of 5th International Conference on Advances in Power System Control, Operation and Management APSCOM 2000*, Hong Kong, October 2000.
8. Lee, C.-H., Wang, Y.-J., and Haung, W.-L., "A literature survey of wavelets in power engineering applications," *Proceedings of National Counc. ROC (A)*, Vol. 24, No. 4, 2000.
9. Darwish, H. A., Maxoud, A., and Taalab, I., "Development and implementation of ANN-based fault diagnosis scheme for generator winding protection," *IEEE Trans. on Power Delivery*, Vol. 16, No. 2, pp. 208–214, April 2001.
10. Nengling, T., Zhijian, H., Xianggen, Y., Xiaohua, L., and Deshu, C., "Wavelet-based ground fault protection scheme for generator stator winding," *Electric Power System Research*, Vol. 62, pp. 21–28, 2002.